The Reaction of Alkyl Hydropersulfides (RSSH, R = CH_3 and ^tBu) with H_2S in the Gas Phase and in Aqueous Solution

Linxing Zhang,[†,‡] Xinhao Zhang,[†] Yun-Dong Wu,[*,†,§]

Yaoming Xie,[‡] Jon M. Fukuto[∥] and Henry F. Schaefer III[*,‡]

[†]*Lab of Computational Chemistry & Drug Design, State Key Laboratory of Chemical Oncogenomics, Peking University Shenzhen Graduate School, Shenzhen 518055, China*

[‡]*Center for Computational Quantum Chemistry, University of Georgia, Athens, GA 30602, USA.*

[§] *College of Chemistry and Molecular Engineering, Peking University, Beijing 100871, China*

[∥] *Department of Chemistry, Sonoma State University, Rohnert Park, CA 94928, USA*

wuyd@pkusz.edu.cn (Y. W.), ccq@uga.edu (H. F. S.)

Abstract: The RSSH + H_2S → RSH + HSSH reaction has been suggested by numerous labs to be important in H_2S-mediated biological processes. Seven different mechanisms for this reaction (R = CH_3, as a model) have been studied using the DFT methods (M06-2X and ωB97X-D) with the Dunning aug-cc-pV(T+d)Z basis sets. The reaction of CH_3SSH with gas phase H_2S has a very high energy barrier (> 45 kcal/mol), consistent with the available experimental observations. A series of substitution reactions R^1–S–S–H + $^-$S–R^2 (R^1 = Me, ^{t}Bu, Ad, R^2 = H, S–Me, S–^{t}Bu, S–Ad) have been studied. The regioselectivity is largely affected by the steric bulkiness of R^1, but is much less sensitive to R^2. Thus, when R^1 is Me, all $^-$S–R^2 favorably attack the internal S atom, leading to R^1–S–S–R^2. While for R^1 = ^{t}Bu, Ad, all $^-$S–R^2 significantly prefer to attack the external S atom to form $^-$S–S–R^2. These results are in good agreement with the experimental observations.

1. Introduction

In 1996 hydrogen sulfide (H_2S) was suggested by Abe and Kimura as an endogenous neuromodulator in the brain.[1] The endogenous metabolism and physiological functions of H_2S make it the third gasotransmitter, in addition to the previously known gasotransmitters nitric oxide (NO) and carbon monoxide (CO).[2] H_2S has also been found to play an important role in cellular functions. It acts as a relaxant of smooth muscle and as a vasodilator.[3] It is also active in the brain, altering hippocampal long-term potentiation, which is involved in the formation of memory.[4]

Much of H_2S signaling has been proposed to occur through modification of cysteine residues in proteins leading to the formation of hydropersulfides (-SSH groups),[5] and this modification has been referred to as S-sulfhydration (or more appropriately, sulfuration or S-persulfidation). The S-sulfuration process can be a post-translational modification of specific proteins that regulate protein functions leading to either activation or inhibition of protein activity,[6] and thus S-sulfuration can serve an important cellular regulatory role.[7] It was found by mass spectrometry that, besides protein hydropersulfides, small molecule hydropersulfides such as cysteine hydropersulfide (CysSSH) and glutathione hydropersulfide (GSSH) are formed in mammalian cells and tissues.[8] Some of the small molecule hydropersulfides are likely to be key intermediates in protein S-sulfuration. For example, polysulfide compounds, such as diallyl trisulfide,[9] penicillamine-derived acyl disulfides,[10] and dithioperoxyanhydride[11] reacted with cysteine or glutathione *in vivo*.

However, since hydropersulfides are usually unstable species, especially in aqueous solution,[12] only a limited number of small molecule hydropersulfides have been synthesized and characterized, although the first hydropersulfide was prepared as early as 1954.[13] In recent years, many experimental studies of the reactivity of hydropersulfides have used hydropersulfides generated *in situ* rather than isolated persulfides.[14] For example, Francoleon and coworkers studied protein hydropersulfides generated via the reaction of H_2S with the papain-cysteine mixed disulfide (Papain–S–S–Cys) as the reactant.[14a] This reaction yielded inactive papain

persulfide (Papain–SSH) via

$$\text{Papain–S–S–Cys} + H_2S \rightarrow \text{Papain–SSH (inactive)} + \text{Cys–SH} \quad (1)$$

With excess H_2S, the inactive persulfide intermediate (Papain–SSH) was converted to the active thiol species (Papain–SH). This observation, the H_2S-mediated generation of active thiol from the hydropersulfide, is consistent with the reaction of RSSH with H_2S giving the presumed products thiol and hydrogen persulfide (H_2S_2)

$$RSSH + H_2S \rightarrow RSH + H_2S_2 \quad (2)$$

Recently, Bailey, Zakharov, and Pluth carried out experimental studies on a series of reactions of hydropersulfides with different reagents.[15] Their experimental results showed that no reaction was observed when RSSH was treated with gas-phase H_2S, while different products were found when RSSH with different R substituent groups reacted under the presence of various nucleophiles and bases in CD_2Cl_2 at room temperature. In essense, Trt–S–SH and Ad–S–SH lead to the formation of Trt–SH and Ad–SH, respectively, accompanied with the formation of S_8. Bn–S–SH, on the other hand, reacted under various conditions to form polysulfides.

In order to understand and provide insight into the reactions of RSSH with H_2S or HS^-, and R–S–S^-. in the present paper we perform theoretical studies to predict the mechanisms for these reactions under various conditions. Our theoretical results will be compared with available experiments, and may further shed light on the function of H_2S as a signaling molecule in biochemical systems.

2. Computational Details

Density functional theory (DFT) methods were employed, providing an approximate treatment of electron correlation effects. Two popular functionals adopted in the present study are M06-2X, which is a meta-GGA functional recommended by Zhao and Truhlar for the study of main-group thermochemistry and kinetics,[16] and ωB97X-D, which including empirical atom-atom dispersion corrections reported by Chai and Head-Gordon.[17] The M06-2X and ωB97X-D computations were performed with the Gaussian09 program package,[18] using the ultrafine integration

grid[19] for geometry optimizations and vibrational frequency analyses.

Dunning's correlation-consistent triple-zeta basis sets with augmented diffuse functions aug-cc-pVTZ were adopted for the C and H atoms.[20] For the S atom, an additional set of d functions was added, denoted as aug-cc-pV(T+d)Z, which corrects some of the deficiencies of the standard correlation consistent basis sets for the second-row atoms Al - Cl.[21] Solvation effects were taken into account via SMD, the Cramer-Truhlar solvation model based on the charge density.[22] We would prefer to treat the solvent with explicit water molecules, but this is not feasible with our current resources. All structures shown here in figures were generated with the CYLview program.[23]

Since the potential energy surfaces predicted by M06-2X and ωB97X-D are in very good agreement with each other, only the M06-2X results are shown in the figures for clarity, while all DFT results are reported in Tables S1 – S7 (in the Supporting Information) for comparison.

3. Results and Discussion

3.1. Reaction Between CH_3SSH and H_2S in the Gas Phase.

Here we selected R = CH_3 as a reasonable initial model for reaction (2) to perform the DFT study. First, a one-step four-membered ring transition state (**TS1-1** in mechanism 1) was examined, in which the sulfur-hydrogen bond in H_2S and the sulfur-sulfur bond in CH_3SSH are about to break. Simultaneously, the sulfur-sulfur bond and the hydrogen-sulfur bond between the two molecules (H_2S and CH_3SSH) are being formed. In **TS1-1**, the distance of the H–S bond being formed is 1.34 Å, and the distance of the old H–S bond in H_2S increases to 2.64 Å (Figure 1), clearly indicating that a hydrogen atom of H_2S is moving to CH_3SSH. Similarly, the –SH group in CH_3SSH is moving to H_2S (Figure 1). Intrinsic reaction coordinate (IRC) analysis shows that the transition state **TS1-1** connects the two complexes (the IRC plot and representative structures along the reaction coordinate are shown in the Supporting Information). The reactant complex **INT1-1** has an H···S hydrogen bond (2.81 Å) between one H atom in H_2S and the internal S atom in CH_3SSH. **INT1-1** lies lower

than the reactant (H_2S and CH_3SSH) by 3.2 kcal/mol. The product complex **INT1-2** has a hydrogen bond (2.64 Å) between one H atom in HSSH and the internal S atom in CH_3SH. **INT1-2** lies lower than the products (HSSH and CH_3SH) by 4.6 kcal/mol. Reaction (1) is endothermic by 3.8 kcal/mol. However, for Mechanism 1 the energy barrier (61.8 kcal/mol in electronic energy and 73.8 kcal/mol in the Gibbs free energy) is very high, suggesting that this mechanism is not feasible.

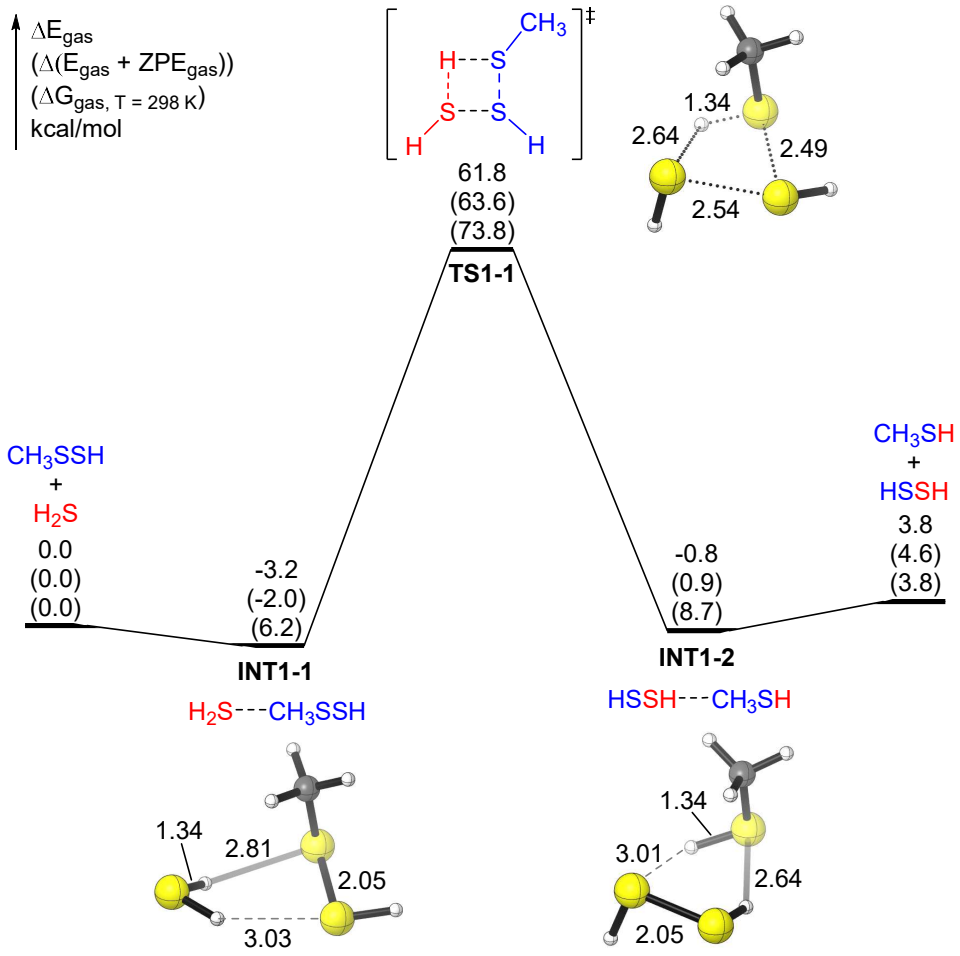

Figure 1. Sketch of the potential energy surface of **Mechanism 1** for the CH_3SSH + H_2S reaction. The relative energies after ZVPE correction (ΔE_{ZVPE}) and the free energies at 298 K (ΔG_{298}) are shown in parentheses. It is seen that entropy plays a significant role for **INT1-1**, **TS1-1**, and **INT1-2**.

The second pathway in the gas phase (Mechanism 2) is shown in Figure 2. In this pathway, one H atom in H_2S attacks the internal S atom in CH_3SSH, and the

remaining SH group approaches the external S atom in RSSH (Figure 2). The IRC analysis shows that the transition state **TS2-1** also connects two complexes. The reactant complex **INT2-1**, similar to **INT1-1** in Figure 1, has a hydrogen bond (H···S distance 2.80 Å) between one H atom in H_2S and the internal S atom in CH_3SSH. The other H atom in H_2S points in the opposite direction. **INT2-1** lies lower than the reactant (H_2S and CH_3SSH) by 2.8 kcal/mol (Figure 2). The product complex **INT2-2** does not have an obvious hydrogen bond, and **INT2-2** lies lower than the products (HSSH plus CH_3SH) by only 1.7 kcal/mol. Again, the energy barrier for Mechanism 2 is too high (67.3 kcal/mol in electronic energy and 77.8 kcal/mol in the Gibbs free energy), suggesting that this reaction in the gas phase will not take place at room temperature.

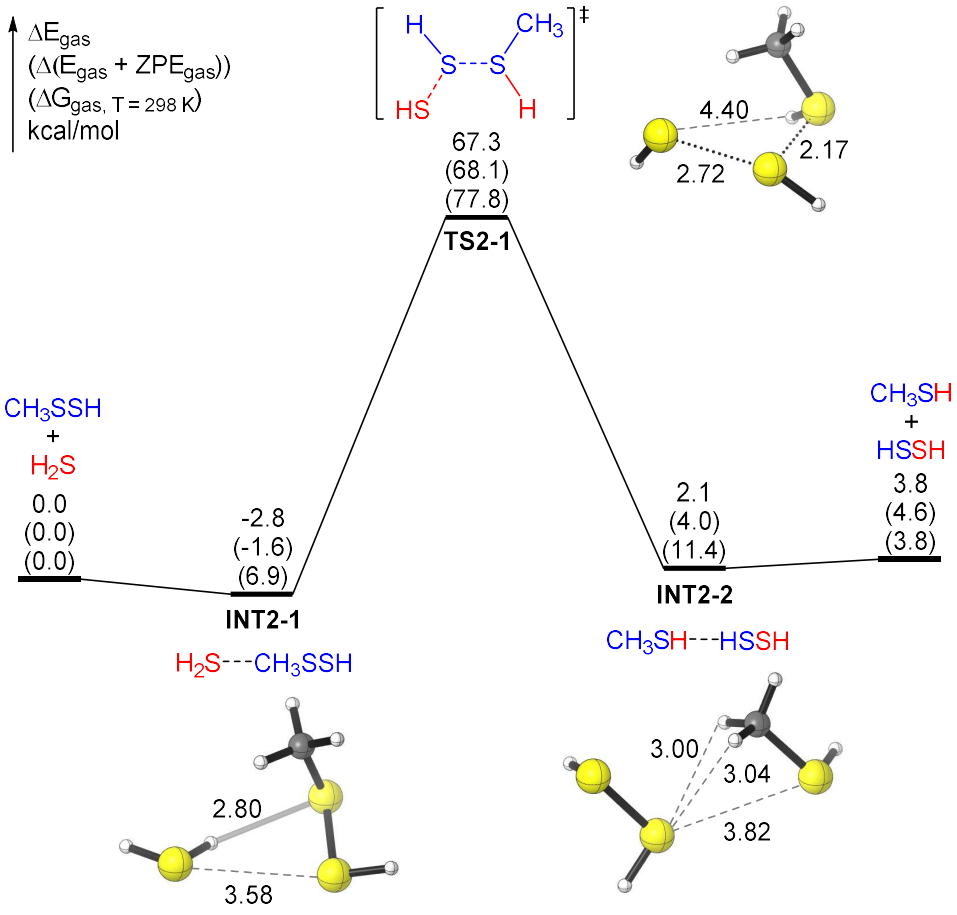

Figure 2. The potential energy surface of **Mechanism 2** for the $CH_3SSH + H_2S$ reaction. The relative energies after ZVPE correction (ΔE_{ZVPE}) and the free energies at 298 K

(ΔG_{298}) are shown in parentheses.

It was reported by mass spectrometry in 2000 by Gerbaux *et al.*[24] that the thiosulfoxide species (R_2SS, R = H, CH_3, C_2H_5), which are tautomers of the disulfides (RSSR), are stable in the gas phase. The transition states for the tautomerizations between disulfides (RSSR) and thiosulfoxides (R_2SS) have been considered in previous theoretical studies.[24-25] The thiosulfoxides RS(=S)H could be regarded as "singlet sulfur" sulfanes that are very electrophilic, and would be more reactive with H_2S.[6, 12a] Thus, a two-step mechanism (Mechanism 3) was explored in the present study (Figure 3). The first step is the tautomerization from the persulfide CH_3SSH to its thiosulfoxide tautomer $CH_3S(=S)H$ (**INT3-1**), which lies above CH_3SSH by 21 kcal/mol. The energy barrier for this tautomerization is predicted to be 44 kcal/mol (**TS3-1**). Following the tautomeric step is the nucleophilic attack by H_2S. In that transition state (**TS3-2**), the sulfur-sulfur bond between H_2S and $CH_3S(=S)H$ is being formed (2.41 Å), while the sulfur-sulfur bond in $CH_3S(=S)H$ is breaking (increasing to 2.53 Å). In the meantime, the proton in H_2S is being transferred to the negatively charged (in terms of a Lewis structure) external sulfur of $CH_3S(=S)H$ (Figure 3). Although Mechanism 3 has a lower overall energy barrier (46.0 kcal/mol in electronic energy and 54.8 kcal/mol in the Gibbs free energy) than Mechanism 1 or Mechanism 2, this barrier is still too high for Reaction (1) to proceed.

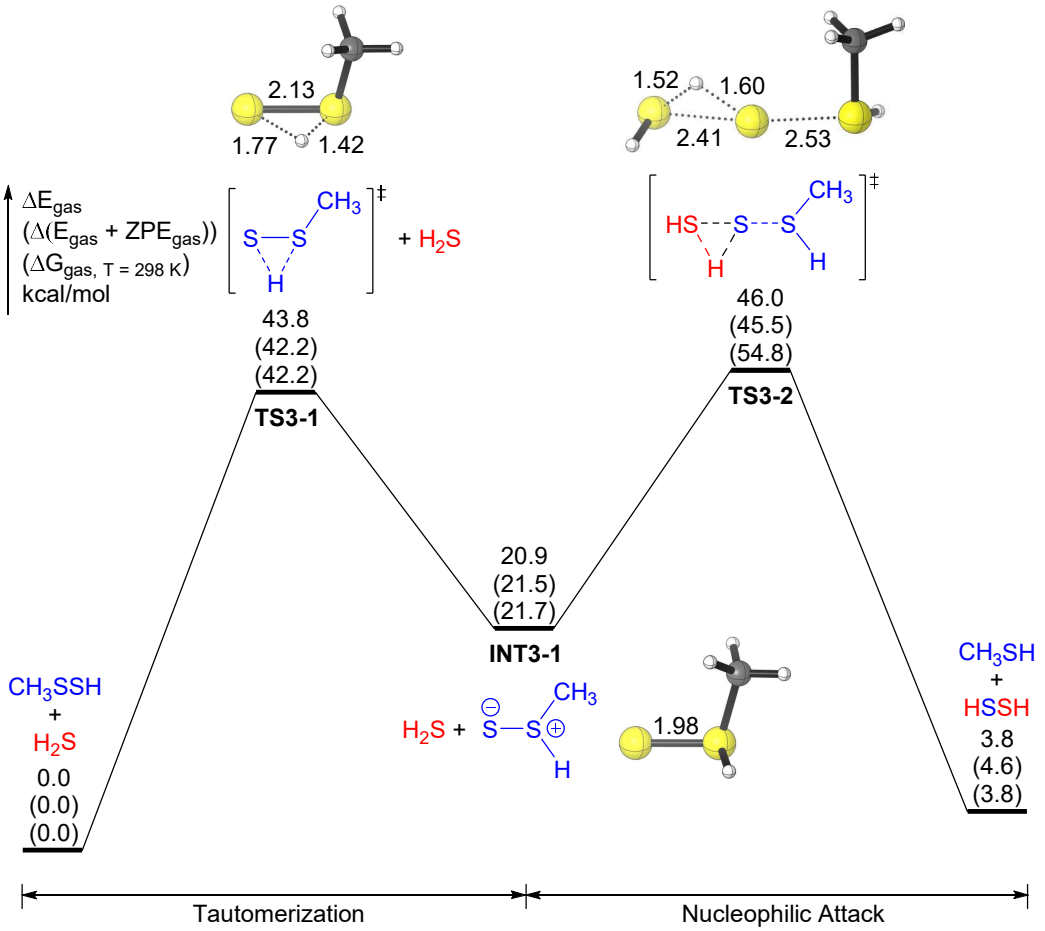

Figure 3. A two-step potential surface (**Mechanism 3**) for the $CH_3SSH + H_2S$ reaction. The relative energies after ZVPE correction (ΔE_{ZVPE}) and the free energies at 298 K (ΔG_{298}) are shown in parentheses.

3.2. Reaction Between CH_3SSH and H_2S in Solvent.

The high energy barriers of the above mechanisms indicate that the $CH_3SSH + H_2S$ reaction in the gas phase is unfavorable. This is consistent with the experimental facts reported by Pluth and co-workers.[15] They studied the reactivity of a series of persulfides in the presence of gas phase H_2S, and found that no reaction happened for benzyl hydropersulfide (BnSSH), trityl hydropersulfide (TrtSSH), or adamantyl hydropersulfide (AdSSH).

It is known that proton transfer steps are often facilitated by solvation in water, and the solvent effect may be very important for Reaction (2). However, for Reaction (2) in aqueous solution, either hydropersulfide or H_2S may ionize depending on their

acidity. To compare the deprotonation abilities of CH_3SSH and H_2S, at first we studied the following reaction with the SMD solvation model[22]

$$CH_3SSH + HS^- \rightarrow CH_3SS^- + H_2S \qquad (3)$$

This reaction energy ΔE for (3) is -0.4 kcal/mol, and the corresponding ΔG_{298} is -1.5 kcal/mol, revealing that CH_3SSH is more acidic than H_2S in water. This is consistent with previous studies.[12a, 26]

In light of the differences in acidities between a hydropersulfide and H_2S, the reactants in the aqueous solution model are CH_3SS^- and H_2S. The main feature of the potential energy surface for the reaction of $CH_3SS^- + H_2S \rightarrow CH_3SH + HSS^-$ is illustrated in Figure 4. The reaction begins with a barrierless formation of a reactant complex **INT4-1** ($CH_3SS^-\cdots HSH$), which is predicted to lie below the reactants ($CH_3SS^- + H_2S$) by 5.4 kcal/mol. Subsequently the reactant complex experiences a small energy barrier (**TS4-1**, 3.2 kcal/mol) for proton transfer to form a second complex $CH_3SSH\cdots SH^-$ (**INT4-2**), leading to the activation of the nucleophile. The HS^- moiety in **INT4-2** then undergoes a nucleophilic attack on the external S atom of CH_3SSH, over an energy barrier of 14.0 kcal/mol (**TS4-2**), to form the intermediate $CH_3S^-\cdots S(H)SH$ (**INT4-3**). A very quick proton transfer from the HSSH moiety to the CH_3S^- part follows, forming the product complex $CH_3SH\cdots SSH^-$ (**INT4-4**). The release of the final products ($CH_3SH + HSS^-$) from the complex **INT4-4** requires 5.1 kcal/mol energy. The overall Reaction (3) is endothermic by 2.5 kcal/mol, and the overall barrier is only 15.0 kcal/mol (20.6 kcal/mol in the Gibbs free energy), which makes this reaction feasible in aqueous solution.

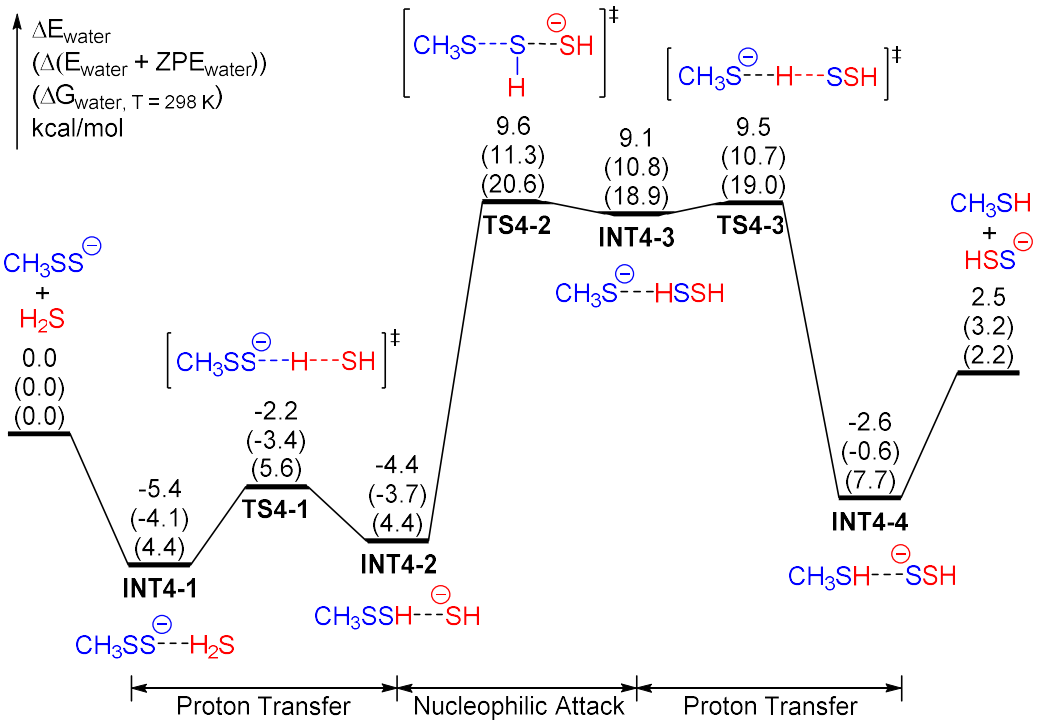

Figure 4. The potential energy surface (**Mechanism 4**) for the CH_3SS^- + H_2S → CH_3SH + HSS^- reaction in aqueous solution. The relative energies after ZVPE correction (ΔE_{ZVPE}) and the free energies at 298 K (ΔG_{298}) are shown in parentheses.

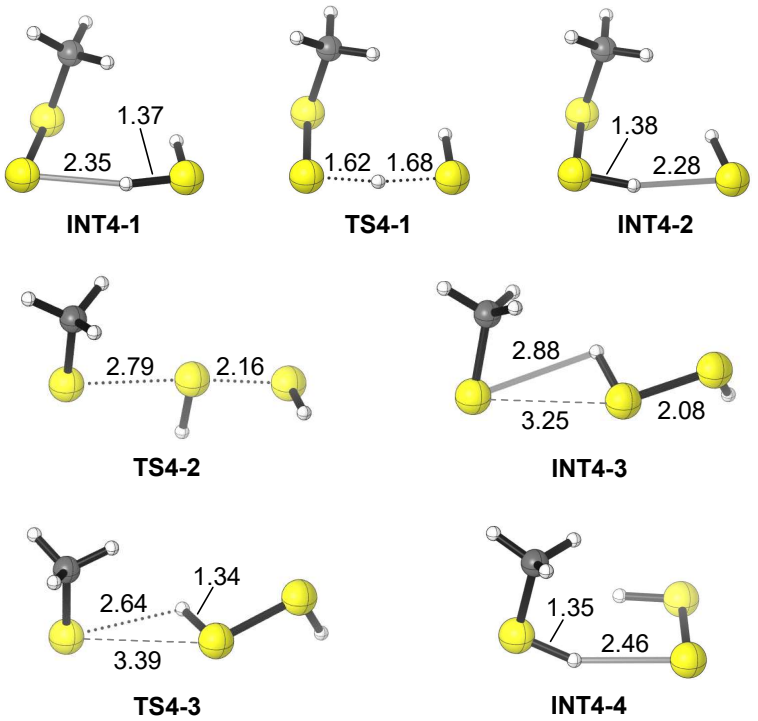

Figure 5. The geometries for the stationary points in Figure 4.

Inspired by proposed mechanisms in which thiols react with disulfides via α carbon nucleophilic attack,[9a, 27] an alternative mechanism for the reaction between CH_3SS^- and H_2S was taken into account (Mechanism 5, Figure 6). After the formation of **INT4-2**, which follows that in Mechanism 4, the nucleophilic attack of HS^- can take place at the α-C atom of CH_3SSH as an S_N2 reaction to give the final products (CH_3SH + HSS^-). The energy barrier with respect to the lowest-lying structure for Mechanism 5 is 35.2 kcal/mol (**TS5-2**) (39.4 kcal/mol in the Gibbs free energy), which is much higher than that for Mechanism 4. Related results were reported in a 2017 theoretical study,[27] which showed that nucleophilic attacks on the α-C atoms of disulfides (RSSR) and trisulfides (RSSSR) involve higher barriers than that on the S atoms.

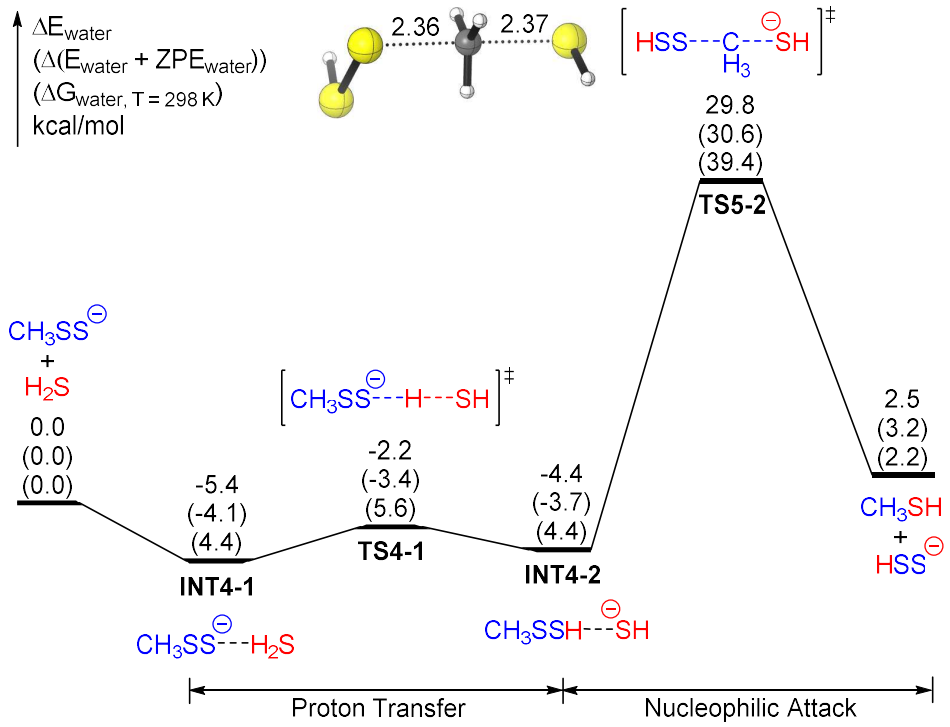

Figure 6. The potential energy surface (**Mechanism 5**) for the $CH_3SS^- + H_2S \rightarrow CH_3SH + HSS^-$ reaction in aqueous solution. The relative energies after ZVPE correction (ΔE_{ZVPE}) and the free energies at 298 K (ΔG_{298}) are shown in parentheses.

3.3. Further Explorations: Adding RSS^- to the Brew

The product HSS^-, predicted by the Mechanisms 4 and 5, was not observed in the 2015 experiments of Bailey and Pluth.[15b] This may be because HSS^- is not an isolable species, but able to further react to give H_2S and elemental sulfur.[12b] However, the experiments show that different products were observed when different RSSH molecules were treated with $[NBu_4^+][HS^-]$,[15b] giving a hint that some competitive mechanisms may exist. Therefore, additional possible mechanisms involving different nucleophiles should be explored. Since the reactant RSS^- has been reported to be a nucleophile,[12b, 28] it could react with hydropersulfides. The target of the nucleophilic attack of RSS^- could be either of the two S atoms in RSSH, leading to two possible mechanisms. The target of the α-C atom in RSSH is less plausible and will not be considered, as it may be similar to the case of Mechanism 5, compared with Mechanism 4.

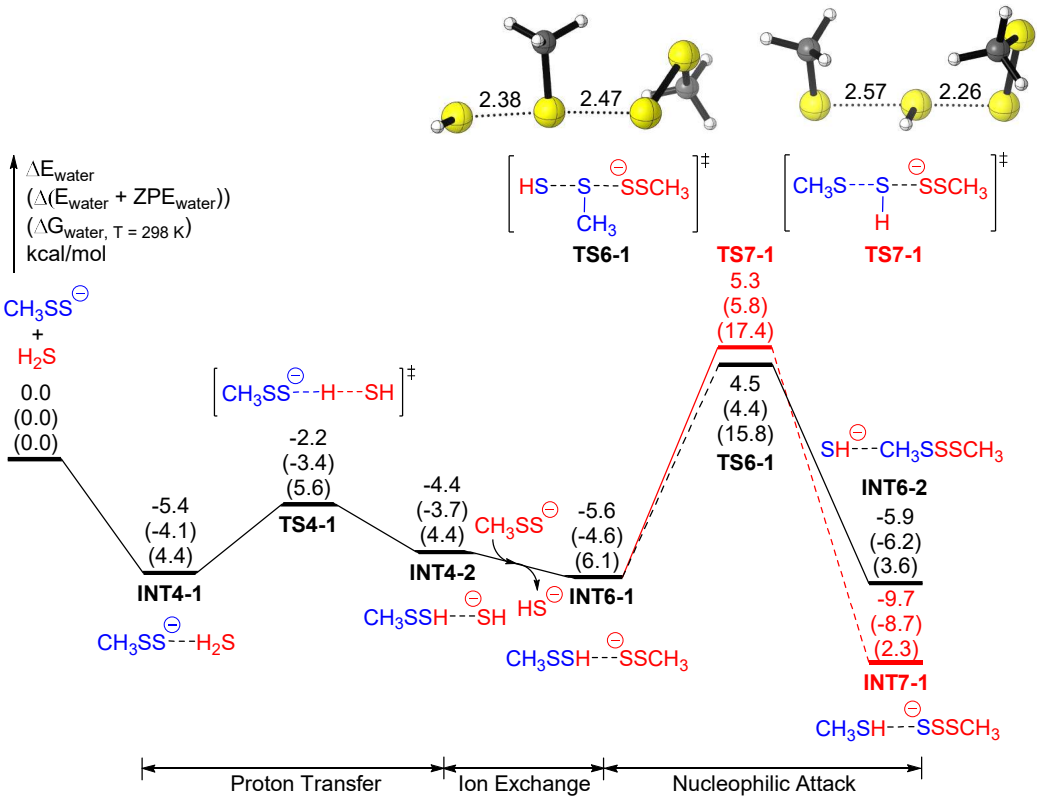

Figure 7. Sketch of the PESs for **Mechanisms 6** and **7** for the reaction of CH_3SS^- and H_2S when the intermediate CH_3SSH is attacked by the additional nucleophile CH_3SS^-. The aqueous solution is taken into count. The relative energies after ZVPE correction (ΔE_{ZVPE}) and the free energies at 298 K (ΔG_{298}) are shown in parentheses. Note that the left section of this sketch is the same as that shown in Mechanisms 4 and 5. In order to keep the PESs continuous before and after the ion exchange, additional energy of CH_3SS^- is added before the ion exchange, and additional energy of HS^- is added after the exchange.

Starting from the complex **INT4-2** ($CH_3SSH\cdots SH^-$ in Mechanisms 4 and 5), a more thermodynamically favorable complex $CH_3SSH\cdots{}^-SSCH_3$ (**INT6-1**) is found to combine with CH_3SS^- and release HS^- (Figure 7). Then the CH_3SS^- moiety in **INT6-1** may attack the CH_3SSH moiety at either the internal S atom or the external S atom. In the former case (Mechanism 6, black line in Figure 7), it goes over a transition state (**TS6-1**) with a barrier of 10.1 kcal/mol to produce $CH_3SSSCH_3\cdots HS^-$ (**INT6-2**), releasing an energy of 0.3 (5.9 – 5.6) kcal/mol. In the latter case (Mechanism 7, red line

in Figure 7), it goes over a transition state (**TS7-1**) with a slightly higher energy barrier (10.9 kcal/mol) but to produce $CH_3SH\cdots SSSCH_3^-$ (**INT7-1**), which is lower than **INT6-2** by 3.8 (9.7 – 5.9) kcal/mol. Figure 7 shows that Mechanism 6 (black line) is a kinetically favored mechanism, while Mechanism 7 (red line) is a thermodynamically favored mechanism. A similar case was earlier considered for the nucleophilic reaction of CN^- and RSSH,[29] in which the nucleophilic attack by CN^- onto the internal sulfur atom of RSSH is kinetically favored, while attack on the external sulfur atom is thermodynamically favored.

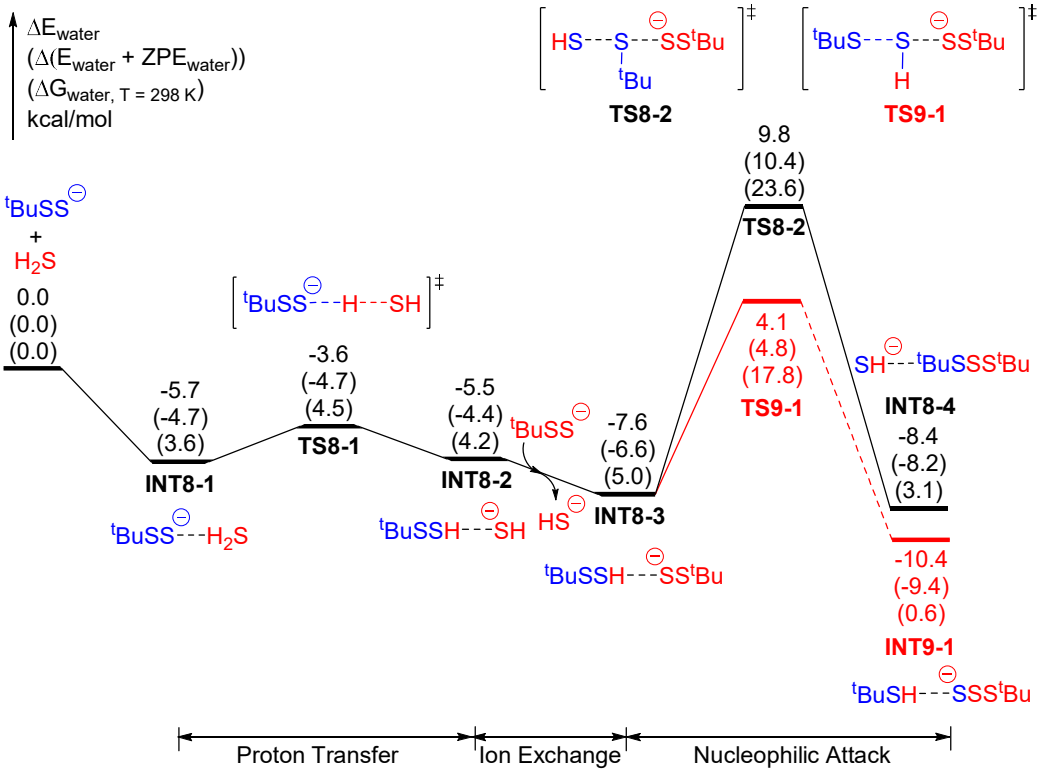

Figure 8. The PESs for the reaction of $^tBuSS^-$ and H_2S in aqueous solvent. The relative energies after ZVPE correction (ΔE_{ZVPE}) and the free energies at 298 K (ΔG_{298}) are shown in parentheses. In order to keep the PESs continuous before and after the ion exchange, additional energy of $^tBuSS^-$ is added before the ion exchange, and additional energy of HS^- is added after the exchange.

As described above, the products of the reactions between RSSH and $[NBu_4^+][HS^-]$

depend on the R groups. For example, when BnSSH (benzyl persulfide) reacts with $[NBu_4^+][HS^-]$ the products were reported to be H_2S and polysulfides (mainly BnSSSBn),[15b] and this corresponds to Mechanism 6 (black line in Figure 7). When TrtSSH (trityl persulfide) reacts with $[NBu_4^+][HS^-]$, the products were reported to be TrtSH, S_8, and H_2S.[15b] Since H_2S and elemental sulfur could be obtained from the further reaction of RSS^-,[12b] this reaction may correspond to Mechanism 7 (red line in Figure 7). For the same RSSH + HS^- reaction, why did the reactants with different R groups, such as BnSSH and TrtSSH, go through different mechanisms? Is it because of steric hindrance as a function of the group size? For those with less sterically-hindered groups, such as BnSSH, it may be less difficult to attack the internal sulfur atom (via Mechanism 6); while for those with the more sterically-hindered groups, such as TrtSSH, it may be more likely to attack the external sulfur atom (via Mechanism 7).

To verify this conjecture, we carried out a parallel study on another model persulfide with a larger R group, namely, tert-butyl persulfide (^{t}BuSSH), for comparison with the above study of CH_3SSH. The potential surfaces for the nucleophilic attack of ^{t}BuSS$^-$ onto ^{t}BuSSH are shown in Figure 8. Indeed, the energy barriers for the two mechanisms are reversed in comparison with those in Figure 7. For the smaller methyl group, the nucleophilic attack at the internal sulfur atom of RSSH has the lower energy barrier (10.1 kcal/mol vs 10.9 kcal/mol). For the larger tert-butyl group, the nucleophilic attack at the external sulfur atom of RSSH has a lower energy barrier (11.7 kcal/mol vs 17.4 kcal/mol). This comparison shows that the regio-selectivity depends on the R group size in RSS^-, and this is consistent with the experimental results for BnSSH and TrtSSH.

To have a more complete understanding of the reactivities and selectivities of various reactions, we carried out a systematic study as shown in Scheme 1. The computed activation free energies are given in Table 1. The results may be summarized as follows:

1. $^-$S–S–R groups are intrinsically more reactive than $^-$SH, despite of the steric effect of R.

2. When R^1 is a methyl group (representing a primary alkyl), $^-S–R^2$ all prefer to attack the internal S atom. This is because steric effects are not significant, but the formation of ^-SH is more favorable than the formation of $^-S–R^1$.
3. When R^1 is ^{t}Bu or Ad, all $^-S–R^2$ favorably attack the external S atom. In this case, the steric interaction between R^1 and the incoming nucleophile is significant (Scheme 2).
4. The barrier for the attack of nucleophile on the external S atom is not sensitive to the size of the nucleophile $^-S–R^2$.

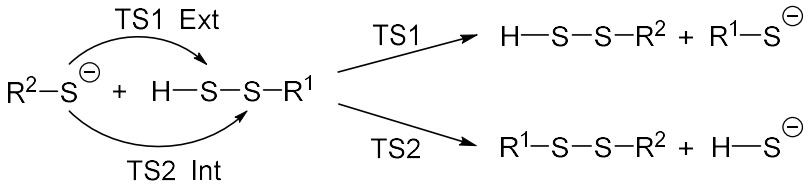

Scheme 1. Two possible pathways of the reaction between $R^2–S^-$ and H–S–S–R^1.

Table 1. Theoretical activation energies (kcal/mol) and Gibbs free energies (in parentheses) of the reactions shown in Scheme 1, using 6-31+G(d) as the basis set.

ΔE_{water} (ΔG_{water})	**R^2 = H**		**R^2 = S–Me**		**R^2 = S–^{t}Bu**		**R^2 = S–Ad**	
	TS1	TS2	TS1	TS2	TS1	TS2	TS1	TS2
R^1 = Me	16.1 (16.5)	13.8 (13.9)	11.0 (11.5)	8.8 (9.2)	10.4 (12.7)	9.5 (11.6)	11.8 (11.6)	11.1 (11.0)
R^1 = ^{t}Bu	17.1 (18.2)	21.1 (21.8)	12.7 (14.6)	17.0 (18.7)	11.8 (12.5)	16.2 (16.6)	13.0 (13.2)	17.9 (18.4)
R^1 = Ad	17.1 (17.6)	21.0 (22.3)	13.8 (12.9)	18.6 (18.4)	12.9 (13.8)	18.1 (18.0)	10.2 (12.1)	16.7 (16.3)

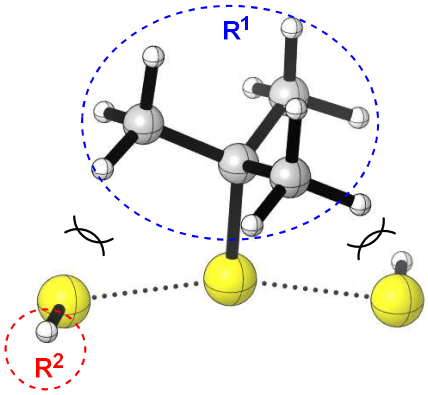

Scheme 2. The steric interaction between R^1 and the incoming nucleophile.

4. Concluding Remarks

We have studied the reaction of RSSH and H_2S, which reaction is suggested to be important in the S-sulfuration process of the gasotransmitter H_2S. Two different DFT methods, M06-2X and ωB97X-D gave similar results, which made us more confident about our results. Our theoretical results predict:

1. The energy barrier for the gas phase reaction $CH_3SSH + H_2S \rightarrow CH_3SH + HSSH$ (Mechanisms 1 – 3) is very high, and in the gas phase this reaction would be unlikely.
2. Although the reaction $CH_3SS^- + H_2S \rightarrow CH_3SH + HSS^-$ (Mechanisms 4 – 5) in aqueous solvent has a lower energy barrier, the product HSS^- is not a favorable species, and other more favorable mechanisms should be explored.
3. CH_3SS^- is a reasonable nucleophile to attack either of the S atoms of CH_3SSH (Mechanisms 6 – 7). Mechanism 6 has a lower energy barrier than mechanism 4, and the products are consistent with the experimental observations.
4. The size of the R group in RSSH will affect the reaction mechanisms. Smaller R groups with less steric hindrance are apt to attack the internal S atom of RSSH (Figure 6), while larger R groups are likely to attack at the external S atom (Figure 7).
5. Our research supports the mechanism for sterically hindered R–S–S–H

proposed by Bayley et al.[15b] For sterically unhindered R–S–S–H, the theory predict the mechanism shown in Scheme 3.

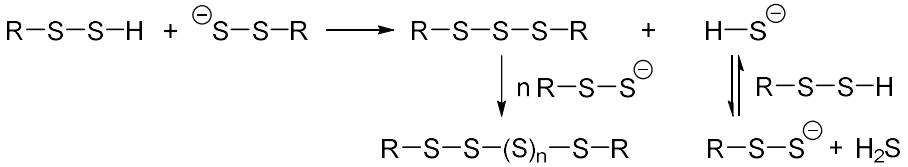

Scheme 3. Mechanism for the reaction of unhindered R–S–S–H.

Acknowledgments

We are grateful for the financial support from the Shenzhen STIC (JCYJ20170412150507046). The research at the Center for Computational Quantum Chemistry was supported by the U.S. National Science Foundation, Grant CHE-1661604.

References

1. Abe, K.; Kimura, H., *J. Neurosci.* **1996,** *16*, 1066.

2. (a) Kabil, O.; Banerjee, R., *J. Biol. Chem.* **2010,** *285*, 21903-21907; (b) Wang, R., *Physiol. Rev.* **2012,** *92*, 791-896; (c) Wang, R. U. I., *FASEB J.* **2002,** *16*, 1792-1798; (d) Wang, R., *Antioxid. Redox Signal.* **2003,** *5*, 493-501.

3. (a) Li, L.; Rose, P.; Moore, P. K., *Annu. Rev. Pharmacool. Toxicol.* **2011,** *51*, 169-187; (b) Lefer, D. J., *Proc. Natl. Acad. Sci. USA* **2007,** *104*, 17907; (c) Yang, G.; Wu, L.; Jiang, B.; Yang, W.; Qi, J.; Cao, K.; Meng, Q.; Mustafa, A. K.; Mu, W.; Zhang, S.; Snyder, S. H.; Wang, R., *Science* **2008,** *322*, 587.

4. Kimura, H., *Mol. Neurobiol.* **2002,** *26*, 13-19.

5. Paul, B. D.; Snyder, S. H., *Nat. Rev. Mol. Cell Biol.* **2012,** *13*, 499.

6. Park, C.-M.; Weerasinghe, L.; Day, J. J.; Fukuto, J. M.; Xian, M., *Mol. BioSyst.* **2015,** *11*, 1775-1785.

7. (a) Krishnan, N.; Fu, C.; Pappin, D. J.; Tonks, N. K., *Sci. Signal.* **2011,** *4*, ra86; (b) Mustafa, A. K.; Sikka, G.; Gazi, S. K.; Steppan, J.; Jung, S. M.; Bhunia, A. K.; Barodka, V. M.; Gazi, F. K.; Barrow, R. K.; Wang, R.; Amzel, L. M.; Berkowitz, D. E.; Snyder, S. H., *Circul. Res.* **2011,** *109*, 1259; (c) Liu, Y.; Yang, R.; Liu, X.; Zhou, Y.; Qu, C.; Kikuiri, T.; Wang, S.; Zandi, E.; Du, J.; Ambudkar, Indu S.; Shi, S., *Cell Stem Cell* **2014,** *15*, 66-78; (d) Mustafa, A. K.; Gadalla, M. M.; Sen, N.; Kim, S.; Mu, W.; Gazi, S. K.; Barrow, R. K.; Yang, G.; Wang, R.; Snyder, S. H., *Sci. Signal.* **2009,** *2*, ra72; (e) Sen, N.; Paul, Bindu D.; Gadalla, Moataz M.; Mustafa, Asif K.; Sen, T.; Xu, R.; Kim, S.; Snyder, Solomon H., *Mol. Cell* **2012,** *45*, 13-24; (f) Yang, G.; Zhao, K.; Ju, Y.; Mani, S.; Cao, Q.; Puukila, S.; Khaper, N.; Wu, L.; Wang, R., *Antioxid. Redox Signal.* **2012,** *18*, 1906-1919.

8. Ida, T.; Sawa, T.; Ihara, H.; Tsuchiya, Y.; Watanabe, Y.; Kumagai, Y.; Suematsu, M.; Motohashi, H.; Fujii, S.; Matsunaga, T.; Yamamoto, M.; Ono, K.; Devarie-Baez, N. O.; Xian, M.; Fukuto, J. M.; Akaike, T., *Proc. Natl. Acad. Sci. USA* **2014,** *111*, 7606-7611.

9. (a) Benavides, G. A.; Squadrito, G. L.; Mills, R. W.; Patel, H. D.; Isbell, T. S.; Patel, R. P.; Darley-Usmar, V. M.; Doeller, J. E.; Kraus, D. W., *Proc. Natl. Acad. Sci. USA* **2007,** *104*, 17977-17982; (b) Liang, D.; Wu, H.; Wong, M. W.; Huang, D., *Org. Lett.* **2015,** *17*, 4196-4199.

10. Zhao, Y.; Bhushan, S.; Yang, C.; Otsuka, H.; Stein, J. D.; Pacheco, A.; Peng, B.; Devarie-Baez,

N. O.; Aguilar, H. C.; Lefer, D. J.; Xian, M., *ACS Chem. Biol.* **2013,** *8*, 1283-1290.

11. Roger, T.; Raynaud, F.; Bouillaud, F.; Ransy, C.; Simonet, S.; Crespo, C.; Bourguignon, M. P.; Villeneuve, N.; Vilaine, J. P.; Artaud, I.; Galardon, E., *ChemBioChem* **2013,** *14*, 2268-2271.

12. (a) Ono, K.; Akaike, T.; Sawa, T.; Kumagai, Y.; Wink, D. A.; Tantillo, D. J.; Hobbs, A. J.; Nagy, P.; Xian, M.; Lin, J.; Fukuto, J. M., *Free Radical Biol. Med.* **2014,** *77*, 82-94; (b) Kawamura, S.; Kitao, T.; Nakabayashi, T.; Horii, T.; Tsurugi, J., *J. Org. Chem.* **1968,** *33*, 1179-1181.

13. (a) Böhme, H.; Zinner, G., *Justus Liebigs Ann. Chem.* **1954,** *585*, 142-149; (b) Nakabayashi, T.; Tsurugi, J., *J. Org. Chem.* **1963,** *28*, 811-813; (c) Tsurugi, J.; Nakabayashi, T.; Ishihara, T., *J. Org. Chem.* **1965,** *30*, 2707-2710; (d) Kawamura, S.; Otsuji, Y.; Nakabayashi, T.; Kitao, T.; Tsurugi, J., *J. Org. Chem.* **1965,** *30*, 2711-2714; (e) Kawamura, S.; Nakabayashi, T.; Kitao, T.; Tsurugi, J., *J. Org. Chem.* **1966,** *31*, 1985-1987; (f) Nakabayashi, T.; Kawamura, S.; Kitao, T.; Tsurugi, J., *J. Org. Chem.* **1966,** *31*, 861-864; (g) Heimer, N. E.; Field, L., *J. Org. Chem.* **1984,** *49*, 1446-1449; (h) Heimer, N. E.; Field, L.; Neal, R. A., *J. Org. Chem.* **1981,** *46*, 1374-1377; (i) Heimer, N. E.; Field, L.; Waites, J. A., *J. Org. Chem.* **1985,** *50*, 4164-4166; (j) Tsurugi, J.; Kawamura, S.; Horii, T., *J. Org. Chem.* **1971,** *36*, 3677-3680.

14. (a) Francoleon, N. E.; Carrington, S. J.; Fukuto, J. M., *Arch. Biochem. Biophys.* **2011,** *516*, 146-153; (b) Millikin, R.; Bianco, C. L.; White, C.; Saund, S. S.; Henriquez, S.; Sosa, V.; Akaike, T.; Kumagai, Y.; Soeda, S.; Toscano, J. P.; Lin, J.; Fukuto, J. M., *Free Radical Biol. Med.* **2016,** *97*, 136-147; (c) Vasas, A.; Dóka, É.; Fábián, I.; Nagy, P., *Nitric Oxide* **2015,** *46*, 93-101.

15. (a) Bailey, T. S.; Zakharov, L. N.; Pluth, M. D., *J. Am. Chem. Soc.* **2014,** *136*, 10573-10576; (b) Bailey, T. S.; Pluth, M. D., *Free Radical Biol. Med.* **2015,** *89*, 662-667.

16. (a) Zhao, Y.; Truhlar, D. G., *Theor. Chem. Acc.* **2008,** *120*, 215-241; (b) Zhao, Y.; Truhlar, D. G., *Acc. Chem. Res.* **2008,** *41*, 157-167.

17. Chai, J.-D.; Head-Gordon, M., *PCCP* **2008,** *10*, 6615-6620.

18. Frisch, M. J.; Trucks, G. W.; Schlegel, H. B.; Scuseria, G. E.; Robb, M. A.; Cheeseman, J. R.; Scalmani, G.; Barone, V.; Mennucci, B.; Petersson, G. A.; Nakatsuji, H.; Caricato, M.; Li, X.; Hratchian, H. P.; Izmaylov, A. F.; Bloino, J.; Zheng, G.; Sonnenberg, J. L.; Hada, M.; Ehara, M.; Toyota, K.; Fukuda, R.; Hasegawa, J.; Ishida, M.; Nakajima, T.; Honda, Y.; Kitao, O.; Nakai, H.; Vreven, T.; Montgomery, J. A., Jr.; Peralta, J. E.; Ogliaro, F.; Bearpark, M.; Heyd, J. J.; Brothers, E.;

Kudin, K. N.; Staroverov, V. N.; Kobayashi, R.; Normand, J.; Raghavachari, K.; Rendell, A.; Burant, J. C.; Iyengar, S. S.; Tomasi, J.; Cossi, M.; Rega, N.; Millam, M. J.; Klene, M.; Knox, J. E.; Cross, J. B.; Bakken, V.; Adamo, C.; Jaramillo, J.; Gomperts, R.; Stratmann, R. E.; Yazyev, O.; Austin, A. J.; Cammi, R.; Pomelli, C.; Ochterski, J. W.; Martin, R. L.; Morokuma, K.; Zakrzewski, V. G.; Voth, G. A.; Salvador, P.; Dannenberg, J. J.; Dapprich, S.; Daniels, A. D.; Farkas, Ö.; Foresman, J. B.; Ortiz, J. V.; Cioslowski, J.; Fox, D. J. Gaussian 09, revision D.01; Gaussian, Inc.: Wallingford, CT, 2016.

19. Wheeler, S. E.; Houk, K. N., *J. Chem. Theory Comput.* **2010,** *6*, 395-404.

20. (a) Dunning, T. H., *J. Chem. Phys.* **1989,** *90*, 1007-1023; (b) Kendall, R. A.; Dunning, T. H.; Harrison, R. J., *J. Chem. Phys.* **1992,** *96*, 6796-6806.

21. Dunning, T. H.; Peterson, K. A.; Wilson, A. K., *J. Chem. Phys.* **2001,** *114*, 9244-9253.

22. Marenich, A. V.; Cramer, C. J.; Truhlar, D. G., *J. Phys. Chem. B* **2009,** *113*, 6378-6396.

23. CYLview, 1.0b; Legault, C. Y., Université de Sherbrooke, 2009 (http://www.cylview.org)

24. Gerbaux, P.; Salpin, J.-Y.; Bouchoux, G.; Flammang, R., *Int. J. Mass spectrom.* **2000,** *195-196*, 239-249.

25. (a) Steudel, R.; Drozdova, Y.; Miaskiewicz, K.; Hertwig, R. H.; Koch, W., *J. Am. Chem. Soc.* **1997,** *119*, 1990-1996; (b) Marsden, C. J.; Smith, B. J., *J. Phys. Chem.* **1988,** *92*, 347-353.

26. Cuevasanta, E.; Lange, M.; Bonanata, J.; Coitiño, E. L.; Ferrer-Sueta, G.; Filipovic, M. R.; Alvarez, B., *J. Biol. Chem.* **2015,** *290*, 26866-26880.

27. Cai, Y.-R.; Hu, C.-H., *J. Phys. Chem. B* **2017,** *121*, 6359-6366.

28. Tsurugi, J.; Abe, Y.; Nakabayashi, T.; Kawamura, S.; Kitao, T.; Niwa, M., *J. Org. Chem.* **1970,** *35*, 3263-3266.

29. Saund, S. S.; Sosa, V.; Henriquez, S.; Nguyen, Q. N. N.; Bianco, C. L.; Soeda, S.; Millikin, R.; White, C.; Le, H.; Ono, K.; Tantillo, D. J.; Kumagai, Y.; Akaike, T.; Lin, J.; Fukuto, J. M., *Arch. Biochem. Biophys.* **2015,** *588*, 15-24.